

F18-fluorodeoxyglucose positron emission tomography in the context of other imaging techniques and prognostic factors in multiple myeloma

Twyla B. Bartel,¹ Jeff Haessler,² Tracy L. Y. Brown,¹ John D. Shaughnessy Jr,³ Frits van Rhee,³ Elias Anaissie,³ Terri Alpe,¹ Edgardo Angtuaco,¹ Ronald Walker,⁴ Joshua Epstein,³ John Crowley,² and Bart Barlogie³

¹Department of Radiology, University of Arkansas for Medical Sciences, Little Rock; ²Cancer Research and Biostatistics, Seattle, WA; ³Myeloma Institute for Research and Therapy, University of Arkansas for Medical Sciences, Little Rock; and ⁴Department of Radiology, Vanderbilt University and Tennessee Valley Veteran's Affairs Healthcare System, Nashville

F18-fluorodeoxyglucose positron emission tomography (FDG-PET) is a powerful tool to investigate the role of tumor metabolic activity and its suppression by therapy for cancer survival. As part of Total Therapy 3 for newly diagnosed multiple myeloma, metastatic bone survey, magnetic resonance imaging, and FDG-PET scanning were evaluated in 239 untreated patients. All 3 imaging techniques showed correlations with prognostically relevant baseline parameters: the number of focal lesions (FLs), especially when

FDG-avid by PET-computed tomography, was positively linked to high levels of β -2-microglobulin, C-reactive protein, and lactate dehydrogenase; among gene expression profiling parameters, high-risk and proliferation-related parameters were positively and low-bone-disease molecular subtype inversely correlated with FL. The presence of more than 3 FDG-avid FLs, related to fundamental features of myeloma biology and genomics, was the leading independent parameter associated with inferior overall and event-free

survival. Complete FDG suppression in FL before first transplantation conferred significantly better outcomes and was only opposed by gene expression profiling-defined high-risk status, which together accounted for approximately 50% of survival variability (R^2 test). Our results provide a rationale for testing the hypothesis that myeloma survival can be improved by altering treatment in patients in whom FDG suppression cannot be achieved after induction therapy. (Blood. 2009;114:2068-2076)

Introduction

The “gold standard” for myeloma imaging has been the metastatic bone survey (MBS), a complete skeletal x-ray technique evaluating the presence of osteolytic disease or osteopenia, the detection of which requires bone decalcification by at least 70%. Diagnostic tools capable of detecting future bone injury at an earlier phase before irreversible lytic changes occur are desirable. Of note, magnetic resonance imaging (MRI) has been shown to permit detection of bone marrow infiltration in a focal, variegated, or diffuse pattern in the absence of bone destruction.¹⁻³

It is well recognized that myeloma engages the microenvironment for its progression by initiating critical survival signals in the process of which bone disease ensues.^{4,5} Through correlative science investigation, we recently reported on Dickkopf-1 (*DKK1*), a novel molecule contributing to myeloma-related bone disease.⁶ By examining global gene expression in purified plasma cells from untreated patients undergoing comprehensive skeletal imaging by both MBS and MRI, we observed a link between MRI-defined focal lesion number (MRI-FL) and *DKK1* expression levels.⁶ Subsequent work revealed an association of MRI-FL with standard prognostic parameters, such as albumin and C-reactive protein (CRP). Survival was adversely affected by MRI-FL independent of the presence of cytogenetic abnormalities (CAs).⁷

F18-fluorodeoxyglucose positron emission tomography integrated with computed tomography (FDG-PET/CT) is a valuable imaging tool in cancer and infection.^{8,9} In addition to the detection

of hypermetabolic tumor, effective suppression early in the course of therapy has been linked to superior patient outcome in lymphoma and a variety of epithelial cancers.¹⁰⁻²⁰ When combined with CT, FDG uptake can be readily localized anatomically and, in the case of myeloma, hypermetabolic activity in intramedullary and extramedullary sites distinguished and osteolytic bone destruction recognized.²¹

As part of Total Therapy 3 (see “Total Therapy 3 program”), we prospectively examined the prognostic implications of FDG-PET/CT and MRI in patients with newly diagnosed myeloma.

Methods

Patient population

Of 303 patients with symptomatic, previously untreated multiple myeloma enrolled in Total Therapy 3 between February 2004 and July 2006, 239 who completed the intended baseline imaging studies are the subjects of this report. All had to have normal cardiopulmonary function, serum creatinine less than 3 mg/dL, and liver function tests within 2 times the upper limit of normal. Zubrod performance status had to be less than 3 unless elevated because of myeloma-related pain. All patients had signed an informed consent in accordance with institutional, and Food and Drug Administration guidelines and the Declaration of Helsinki. The protocol had been approved by the Institutional Review Board of the University of Arkansas for Medical Sciences.

Submitted March 30, 2009; accepted April 28, 2009. Prepublished online as *Blood* First Edition paper, May 14, 2009; DOI 10.1182/blood-2009-03-213280.

An Inside *Blood* analysis of this article appears at the front of this issue.

The publication costs of this article were defrayed in part by page charge payment. Therefore, and solely to indicate this fact, this article is hereby marked “advertisement” in accordance with 18 USC section 1734.

© 2009 by The American Society of Hematology

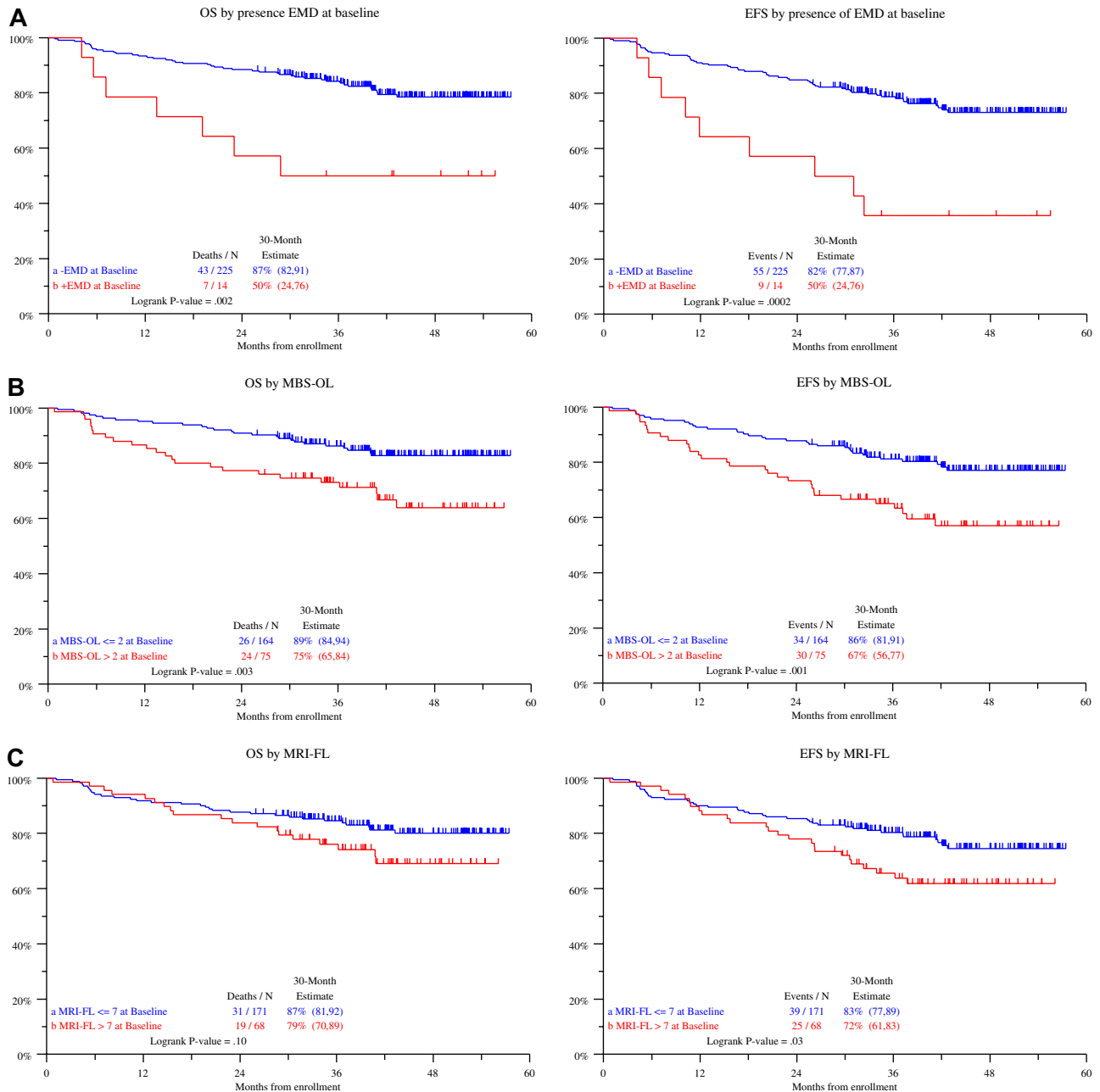


Figure 1. Overall survival and event-free survival and cumulative incidence of complete or near-complete response. (A-E) Overall survival and event-free survival outcomes according to imaging parameters (MBS-OL, MRI-FL, PET-FL, SUV-FL, EMD [cut-points based on tertile distributions and collapsing categories with similar outcomes]): Both overall and event-free survival durations were significantly shorter in the presence of EMD detected on PET examination (A), higher osteolytic lesion number enumerated on metastatic bone survey (MBS-OL; B), and higher focal lesion number on PET (PET-FL; D). Magnetic resonance imaging–defined focal lesions (MRI-FL) conferred inferior event-free survival and a trend toward inferior overall survival (C). Among the overall favorable GEP-defined low-risk group, PET-FL more than 3 identified a subset with inferior outcomes (E). (F-G) Survival outcomes according to complete FDG suppression (100%) before first transplantation: Complete FDG suppression at the end of 2 induction chemotherapy cycles before first transplantation conferred favorable overall and event-free survival (F), which was particularly important for the subset of patients presenting with GEP-defined high-risk features (G). (H) Time course to complete or near-complete response (CR, n-CR; defined by myeloma-protein and bone marrow criteria) and to imaging-defined complete response (resolution of focal lesions on MRI [MRI-CR] and PET [PET-CR], normalization of bone marrow intensity to hypointensity status in patients without MRI-FL): PET-CR status was attained more rapidly than clinical CR or n-CR and especially MRI-CR status among patients presenting with MRI-FL.

Total Therapy 3 program

Total Therapy 3 consisted of 4 distinct phases of induction therapy (2 cycles of VDT-PACE [bortezomib, dexamethasone, thalidomide, and 4-day continuous infusions of cis-platin, doxorubicin, cyclophosphamide, etoposide] with peripheral blood stem cell collection after the first cycle), tandem transplantation with melphalan 200 mg/m² (reduced to 140 mg/m² in case of age > 70 years and creatinine > 2 mg/dL), consolidation with 2 cycles of dose-reduced VDT-PACE, and maintenance therapy for 3 years, with

monthly cycles of VTD for the first year and thalidomide plus dexamethasone in years 2 and 3.²² All patients signed a written informed consent acknowledging the research nature of the study protocol and availability of other treatment options in keeping with the Declaration of Helsinki. According to institutional and federal policies, the protocol was approved by our local Protocol Review and Monitoring Committee and Institutional Review Board. Approximately 80% of patients' records were audited for protocol adherence, toxicity, and response by a federally accredited team of investigators.

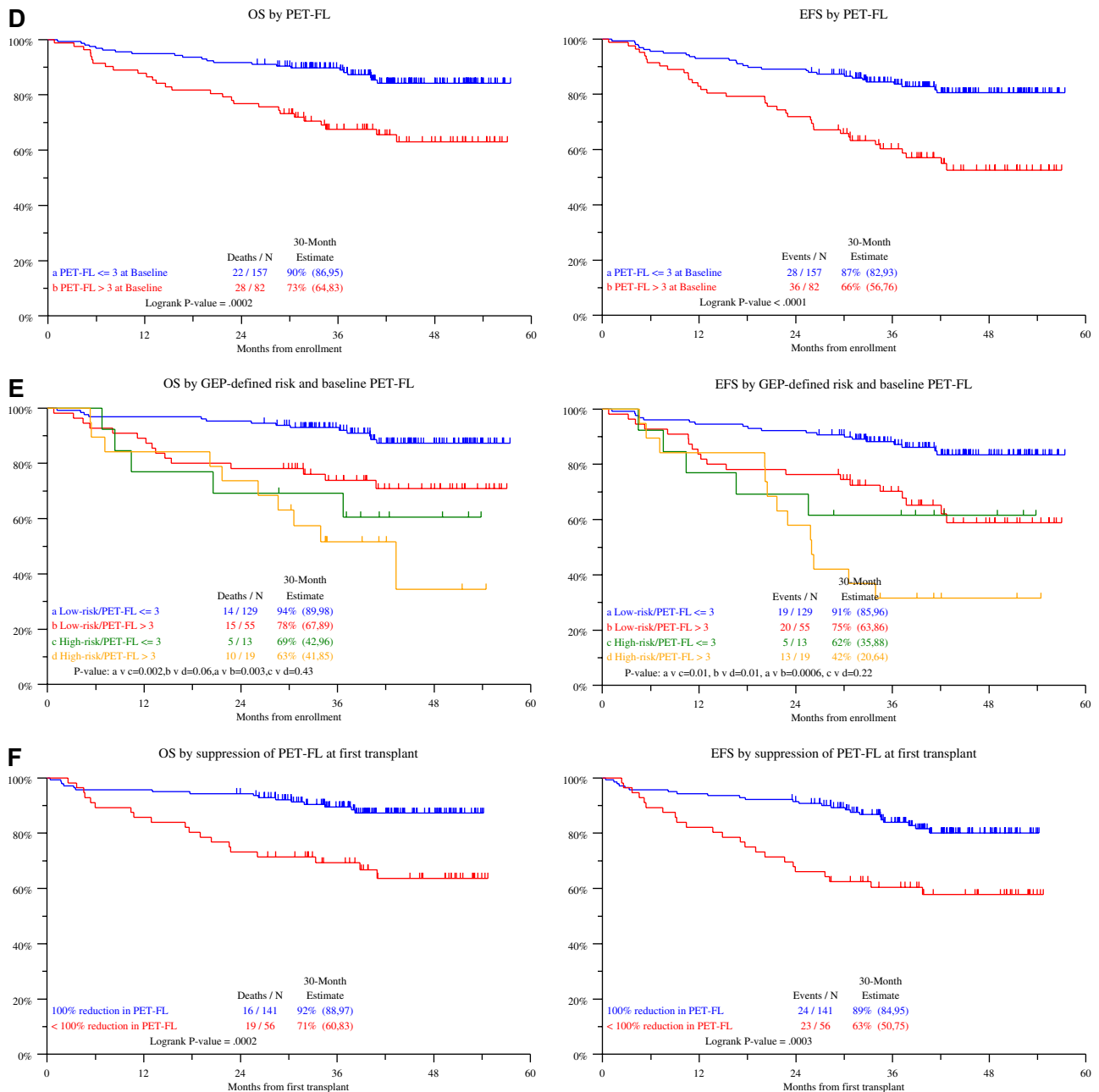


Figure 1 (continued).

Imaging studies

Per study design, all eligible patients had MBS, MRI, and FDG-PET/CT examinations at baseline and at specified subsequent phases of the protocol. The follow-up studies included annual MBS with MRI scans performed before each of 2 transplantations, before consolidation and maintenance phases, and semiannually thereafter. FDG-PET/CT scans were scheduled within 10 days from starting the first induction cycle of VDT-PACE. All imaging studies were repeated at relapse, defined by M-protein and bone marrow criteria and by any of the imaging tools.

Technical details of imaging methods are as follows: MBS consisted of standard digital radiographs of the chest, ribs, lateral skull, vertebral column, anterior and posterior pelvis, shoulders, and extremities to include hands and feet. MRI study sequences, limited to the axial skeleton bone marrow (head, spine, pelvis, shoulders, sternum), included short T1-inversion recovery (STIR-weighted), spin echo (T1- and T2-weighted), gradient-echo (T2), and gadolinium-enhanced spin echo sequences (with and without fat suppression). FDG-PET/CT imaging was performed on 1 of

2 PET/CT scanners: CTI-Reveal or Biograph 6 (Siemens Medical Systems). The CT portion was acquired with a Siemens Sensation helical scanner (Biograph, 6-slice; CTI-Reveal, 16-slice). PET consisted of lutetium oxyorthosilicate crystals arranged in a full-ring gantry (Pico Electronics). Images were obtained 60 minutes after the intravenous administration of 10 to 15 mCi (370-444 MBq) of FDG, and extended from vertex to toes with 4 minutes per bed position. Image reconstruction was performed on a CTI Wizard workstation.

All imaging studies were interpreted by a team of experienced radiologists and nuclear medicine physicians well versed in myeloma diagnostics.

Imaging definitions

Osteolytic lesions on MBS (MBS-OL) were described by location and number. For MRI and PET studies, FL measuring less than 0.5 cm were not included as these are typically below PET/CT resolution despite being identifiable on MRI. In the case of MRI, the marrow signal was described as hyperintense, isointense, or hypointense (in relation to adjacent paraspinal

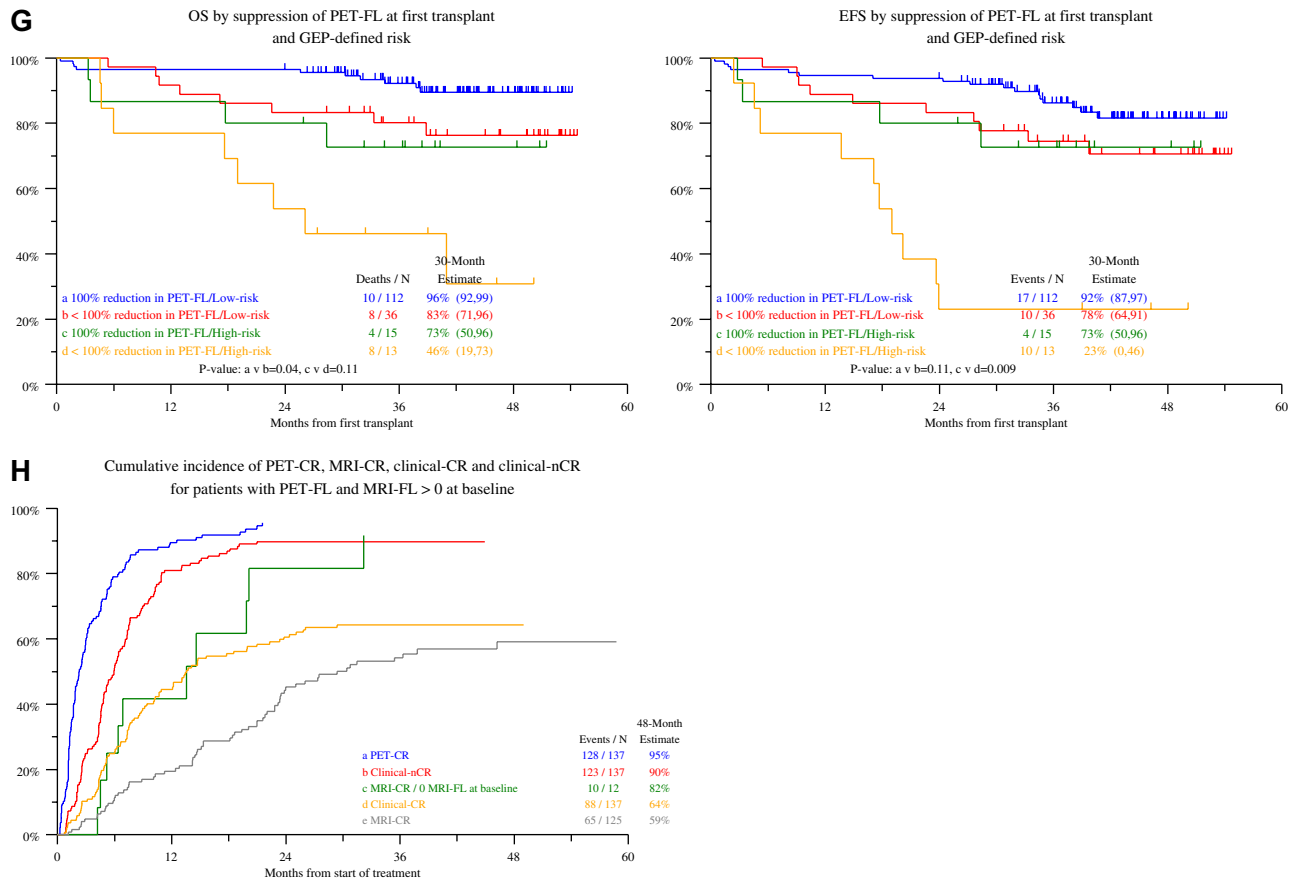


Figure 1 (continued).

musculature on T1 or to normal intervertebral disc signal on STIR images) and also as homogeneous or heterogeneous. MRI-FL (intramedullary) was described by location, number, and size.

Red marrow uptake on PET/CT was described as mild, moderate, or severe in regard to the degree of FDG uptake (determined from the L4 or L5 vertebral body as a standard) and also as homogeneous or heterogeneous regarding pattern of uptake. Hypermetabolic FLs (PET-FLs) were defined as being more intense than background marrow uptake and described by location, number, size, and associated standardized uptake values (SUV-FLs). Intramedullary PET-FLs were considered metabolically active disease, and when resolved, inactive or treated disease. Recorded SUVs were maximum lesion values and calculated based on lean body mass according to standard formula. Extramedullary disease (EMD) was defined as the presence of FDG-avid tissue that, according to CT examination, was not contiguous to bone and arose in soft tissue sites (eg, lymph nodes, liver, pleura, testis, skin). If present, EMD was described by location, size, number, and SUV (SUV-EMD). Occult infection, if detected, was reported.

Osteolytic lesions on CT (CT-OL) were described as to their number independent of the presence of active disease on PET. Size measurements on the imaging studies were to the nearest centimeter as measured on axial views.

Laboratory examinations

As previously reported,²² all eligible patients underwent a comprehensive workup to capture the following myeloma-related parameters: serum M-protein; complete immunoglobulin and free light chain concentrations; daily urinary M-protein excretion; serum levels of beta-2-microglobulin (B2M), CRP, albumin, and lactate dehydrogenase (LDH); bone marrow aspirate and biopsy infiltration by plasma cells along with DNA-cytoplasmic immunoglobulin flow cytometry²³ and cytogenetics.²⁴ Special studies included gene expression profiling (GEP) analyses of CD138-purified plasma cells²⁵ and unseparated bone marrow biopsy samples²⁶ procured from a random posterior iliac crest site or from an MRI- or

PET-defined FL under CT guidance. Risk group and molecular subgroup designations were executed as previously reported.^{27,28}

Definitions of response and relapse

The European Bone Marrow Transplant criteria, introduced by Blade et al, were applied²⁹ and modified by the International Myeloma Working Group.³⁰ Complete response (CR) required the absence of M-protein in serum and urine on immunofixation analysis, whereas near-complete response (n-CR) implied absence of monoclonal bands on standard electrophoresis and presence on immunofixation. Partial response required reductions in serum-M concentration by less than 50% and in urinary M-protein excretion by more than 90% or less than 100 mg/day. In all cases, both bone marrow aspirate and biopsy samples had to be negative for myeloma, implying absence of clonally restricted plasma cells by immunohistochemistry and by 2-parameter flow cytometry of nuclear DNA and cytoplasmic immunoglobulin.²³ These definitions had to apply on at least 2 successive occasions at least 2 months apart. There could not be any new MBS- or CT-OL, MRI- or PET-defined FL, or EMD on PET/CT.

Relapse from CR or n-CR was diagnosed when M-protein became detectable by immunofixation or electrophoresis, respectively. Relapse from partial response implied an increase by more than 50% from the lowest recorded levels. Similarly, relapse was also diagnosed in case of recurrence of monoclonal bone marrow plasmacytosis to more than 5%, increase by more than 50% of residual FL or OL on imaging studies, or the development of new FL, OL, or EMD.

Statistical methods

The Kaplan-Meier method³¹ was used to estimate overall and event-free survival with group comparisons made using the log-rank test.³² Overall survival and event-free survival were measured from the date of registration until death from any cause and disease relapse or death from any cause,

Log odds ratio (OR) and 95% CI for associations with imaging parameters

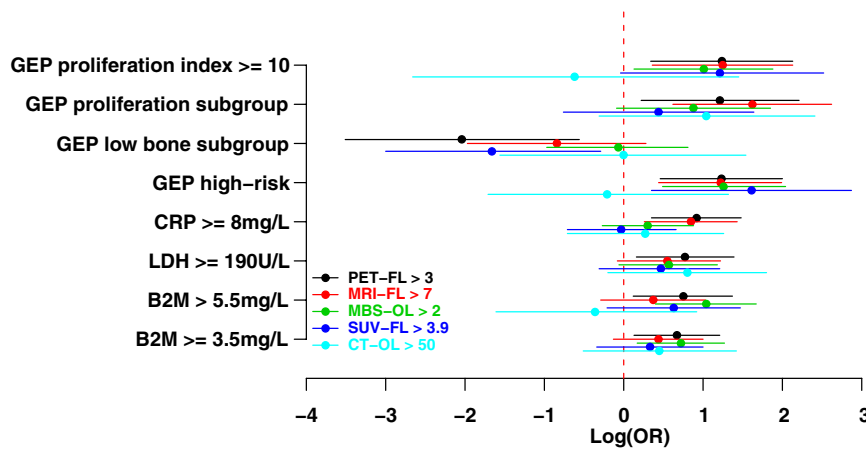


Figure 2. Odds ratio of association of imaging parameters with baseline laboratory and imaging features. Plotted are the log odds ratio values with 95% confidence interval values for 5 imaging parameters (PET-FL, FDG-avid focal lesion number; MRI-FL, MRI-defined focal lesion number; MBS-OL, metastatic bone survey-defined osteolytic lesion number; SUV-FL, maximum standardized uptake values at bone marrow focal lesion sites; CT-OL, computed tomography-defined osteolytic lesion number). Significant correlations were observed for most imaging parameters with B2M, LDH, and several GEP-derived parameters such as high-risk, LB disease and proliferation (PR) subgroups, and proliferation index (PI).

respectively; survivors were censored at the time of last contact. Univariate and multivariate analyses of prognostic factors were carried out using Cox regression.³³ The cumulative incidence of CR was estimated using the method outlined in Gooley et al³⁴ and was compared using the log-rank test. A χ^2 test was used to compare imaging variables in relation to baseline parameters.

Results

Patient characteristics included advanced age (> 65 years) in 28%, hypoalbuminemia (< 3.5 g/dL) in 26%, and elevated B2M to more than 3.5 mg/L in 45% and to more than 5.5 mg/L in 22%. Thirty-two percent were anemic (hemoglobin < 10 g/dL), and 7% had renal insufficiency (creatinine > 2 mg/dL). Serum levels of CRP were more than 8 mg/L in 33%, and LDH was elevated beyond the upper limit of normal in 23%. Metaphase CAs were detected in 34%, whereas 14% had gene array-defined high-risk myeloma.²⁷ The intended therapy involving first and second

transplantation, 2 cycles of consolidation therapy, and at least 1 year of maintenance were completed in 94%, 83%, 77%, and 72%, respectively. With a median follow-up of 43 months, 4-year estimates of overall and event-free survival are 77% and 71%, respectively, and not different from results observed for all 303 patients enrolled in the trial (78% and 71%).

Survival implications of baseline imaging parameters

Applying tertile-derived cut-points (and collapsing similar categories), several imaging parameters affected overall and event-free survival adversely (Figure 1), in particular, the presence of EMD (Figure 1A, $n = 14$) and the number of MBS-OL (Figure 1B) and PET-FL (Figure 1D). MRI-FL (Figure 1C) and SUV-FL (Figure 1E) shortened event-free survival with borderline effects on overall survival. Clinical outcomes were not influenced by CT-OL (not shown). In the context of gene array-defined risk, PET-FL more than 3 conferred inferior overall and event-free survival in the

Table 1. Univariate and multivariate logistic regression analyses of baseline laboratory and imaging parameters associated with the presence of more than 3 FDG-avid focal lesions (PET-FL > 3)

Variable	N	With factor, n (%)	Without factor, n (%)	OR (95% CI)	P*
Univariate model					
B2M \geq 3.5 mg/L	239	46/108 (43)	36/131 (27)	1.96 (1.14-3.36)	.015
B2M > 5.5 mg/L	239	25/52 (48)	57/187 (30)	2.11 (1.13-3.95)	.019
LDH \geq 190 U/L	239	27/56 (48)	55/183 (30)	2.17 (1.17-4.00)	.013
CRP \geq 8 mg/L	238	38/79 (48)	43/159 (27)	2.50 (1.42-4.39)	.001
GEP high-risk	216	19/32 (59)	55/184 (30)	3.43 (1.58-7.42)	.002
GEP LB subgroup	216	2/27 (7)	72/189 (38)	0.13 (0.03-0.57)	.006
GEP PR subgroup	216	11/18 (61)	63/198 (32)	3.37 (1.25-9.10)	.017
GEP proliferation index \geq 10	216	14/23 (61)	60/193 (31)	3.45 (1.41-8.41)	.006
MRI-FL > 7	239	44/68 (65)	38/171 (22)	6.42 (3.47-11.86)	< .001
MBS-OL > 2	239	42/75 (56)	40/164 (24)	3.95 (2.21-7.04)	< .001
Multivariate model					
CRP \geq 8 mg/L	215	34/71 (48)	39/144 (27)	1.98 (1.02-3.84)	.045
GEP LB subgroup	215	2/27 (7)	71/188 (38)	0.14 (0.03-0.65)	.012
MRI-FL > 7	215	37/58 (64)	36/157 (23)	4.09 (2.01-8.32)	< .001
MBS-OL > 2	215	35/66 (53)	38/149 (26)	2.32 (1.16-4.65)	.017

OR indicates odds ratio; CI, confidence interval; B2M, β -2-microglobulin; LDH, lactate dehydrogenase; CRP, C-reactive protein; GEP, gene expression profiling; LB, low bone disease; PR, proliferation; FL, focal lesion; and OL, osteolytic lesion.

*P value from Wald χ^2 test in logistic regression. NS2: Multivariate results not statistically significant at the .05 level. Univariate P values reported regardless of significance. Multivariate model uses stepwise selection with entry level .1, and variable remains if it meets the .05 level. A multivariate $P > .05$ indicates variable forced into model with significant variables chosen using stepwise selection. Other nonsignificant univariate variables include age, albumin, creatinine, hemoglobin, cytogenetic abnormalities, GEP-defined molecular subgroups CD-1, CD-2, HY, MF, MS, MY, and TP53 deletion.

Table 2. Cox regression analyses of baseline laboratory and imaging parameters associated with overall and event-free survival without and with gene array-derived parameters

Model	n/N (%)	Overall survival from start of therapy			Event-free survival from start of therapy		
		HR (95% CI)	P*	R ² , percentage	HR (95% CI)	P*	R ² , percentage
Univariate							
Standard variables							
Age ≥ 65 y	68/239 (28)	1.40 (0.78-2.52)	.258	2.4	1.56 (0.94-2.60)	.088	4.0
Albumin < 3.5 g/dL	62/239 (26)	1.70 (0.95-3.06)	.076	5.7	1.73 (1.03-2.90)	.038	5.5
B2M ≥ 3.5 mg/L	108/239 (45)	1.89 (1.08-3.31)	.027	9.4	1.85 (1.13-3.04)	.015	8.9
B2M > 5.5 mg/L	52/239 (22)	3.14 (1.79-5.51)	< .001	19.1	3.29 (2.00-5.41)	< .001	19.6
Creatinine ≥ 2 mg/dL	17/239 (7)	1.56 (0.62-3.94)	.343	1.4	2.10 (1.00-4.41)	.049	3.7
CRP ≥ 8 mg/L	79/238 (33)	1.59 (0.91-2.79)	.107	4.6	1.51 (0.92-2.49)	.105	3.8
Hb < 10 g/dL	77/239 (32)	1.89 (1.08-3.30)	.025	8.2	1.79 (1.09-2.93)	.021	6.8
LDH ≥ 190 U/L	56/239 (23)	3.02 (1.72-5.31)	< .001	19.5	3.22 (1.96-5.31)	< .001	29.9
Genetic variables							
Cytogenetic abnormalities	82/239 (34)	2.83 (1.62-4.95)	< .001	20.4	2.10 (1.28-3.43)	.003	11.3
GEP high-risk	32/216 (15)	3.61 (1.93-6.75)	< .001	16.6	3.44 (1.96-6.04)	< .001	15.8
Imaging variables							
MRI-FL > 7	68/239 (28)	1.61 (0.91-2.85)	.104	4.4	1.71 (1.04-2.83)	.036	5.6
MBS-OL > 2	75/239 (31)	2.28 (1.31-3.97)	.004	13.1	2.22 (1.36-3.64)	.001	12.2
PET-FL > 3	82/239 (34)	2.79 (1.60-4.88)	< .001	20.2	2.88 (1.76-4.73)	< .001	20.8
CT-OL > 50	18/239 (8)	1.26 (0.45-3.52)	.657	0.6	1.20 (0.48-3.01)	.691	0.4
SUV-FL > 3.9	101/239 (42)	1.74 (1.00-3.04)	.052	7.0	1.78 (1.09-2.92)	.022	7.7
EMD	14/239 (6)	3.26 (1.46-7.24)	.004	7.2	3.54 (1.75-7.18)	< .001	8.1
Multivariate without gene array data†							
Cytogenetic abnormalities	82/238 (34)	2.88 (1.59-5.19)	< .001	20.4	1.85 (1.09-3.13)	.022	11.3
PET-FL > 3	81/238 (34)	2.43 (1.37-4.30)	.002	33.3	2.28 (1.37-3.80)	.002	28.8
LDH ≥ 190 U/L	56/238 (24)	2.04 (1.13-3.68)	.017	42.3	2.00 (1.17-3.42)	.012	36.1
B2M > 5.5 mg/L	52/238 (22)	NS	NS	NS	1.83 (1.05-3.20)	.033	42.0
EMD	14/238 (6)	3.13 (1.34-7.31)	.008	44.5	2.29 (1.05-4.99)	.038	45.7
Multivariate with gene array data†							
Cytogenetic abnormalities	77/215 (36)	2.62 (1.37-5.02)	.004	20.4	1.83 (1.04-3.21)	.036	51.6
PET-FL > 3	73/215 (34)	2.45 (1.30-4.62)	.006	33.3	2.63 (1.51-4.58)	< .001	32.6
LDH ≥ 190 U/L	50/215 (23)	2.28 (1.22-4.28)	.010	37.4	2.38 (1.37-4.13)	.002	20.9
Albumin < 3.5 g/dL	57/215 (27)	2.11 (1.11-4.03)	.023	38.1	2.20 (1.26-3.86)	.006	51.2
GEP high-risk	32/215 (15)	1.76 (0.89-3.50)	.104	44.0	1.86 (1.00-3.44)	.048	46.7

HR indicates hazard ratio; CI, confidence interval; and NS, not statistically significant at the .05 level.

*P value from Wald χ^2 test in Cox regression. Multivariate model uses stepwise selection with entry level .1 and variable remains if it meets the .05 level. Variables considered for stepwise selection include albumin, β -2-microglobulin (B2M), hemoglobin (Hb), lactate dehydrogenase (LDH), C-reactive protein (CRP), cytogenetic abnormalities (CA), and gene expression profiling (GEP) high-risk; imaging parameters include MRI-FL, MBS-OL, PET-FL, SUV-FL, and EMD.

†Data reported in the R² columns for the multivariate models are cumulative. The variable with smallest R² is first to enter model; the next smallest is second to enter; the largest R² is last to enter.

low-risk group, whereas patients with high-risk myeloma all fared poorly (Figure 1F).

Correlations of imaging parameters with laboratory features

The observed prognostic implications may be related to associations of imaging parameters with baseline laboratory features of prognostic significance as examined in Figure 2. Applying tertile distributions of imaging parameters and collapsing pairs with similar associations, significant correlations (expressed as log odds ratio) were observed between PET-FL and all listed standard variables (B2M, LDH, CRP) and all GEP-derived variables (positive links with high-risk and 2 proliferation parameters, inverse correlation with low bone disease subgroup [LB]). MBS-OL was significantly correlated with B2M, gene array-defined high risk, and proliferation index. MRI-FL was linked to CRP as previously reported,⁷ high-risk gene array, and the 2 proliferation parameters. SUV-FL was positively correlated with high risk and inversely linked to LB. CT-OL was not significantly linked to any of the parameters displayed.

Given the prominent correlation of PET-FL with both clinical outcome and prognostic baseline variables, logistic regression analyses were carried out to determine which of the 11 univariately

linked parameters retained significance in a multivariate model (Table 1). MRI-FL and MBS-OL were both independently positively linked to PET-FL along with CRP. Gene array-defined LB was inversely correlated with PET-FL.

Multivariate analysis of baseline variables associated with survival

Twelve of 17 baseline variables examined showed significant outcome implications on univariate analysis (Table 2), of which PET-FL more than 3, LDH elevation, and presence of CA independently conferred inferior overall and event-free survival, both in the absence and presence of gene array data (Table 2). Although pertaining only to 6% of patients, EMD was another adverse variable when gene array information was not included, whereas low albumin levels imparted poor outcomes in the context of molecular genetic data.

Cumulative imaging-defined rates of complete response

Using PET/CT criteria (absence of PET-FL and EMD), CR status was documented in 92% at 18 months, preceding the median onset of clinical n-CR (87%) and CR status (56%) by 4 and 12 months,

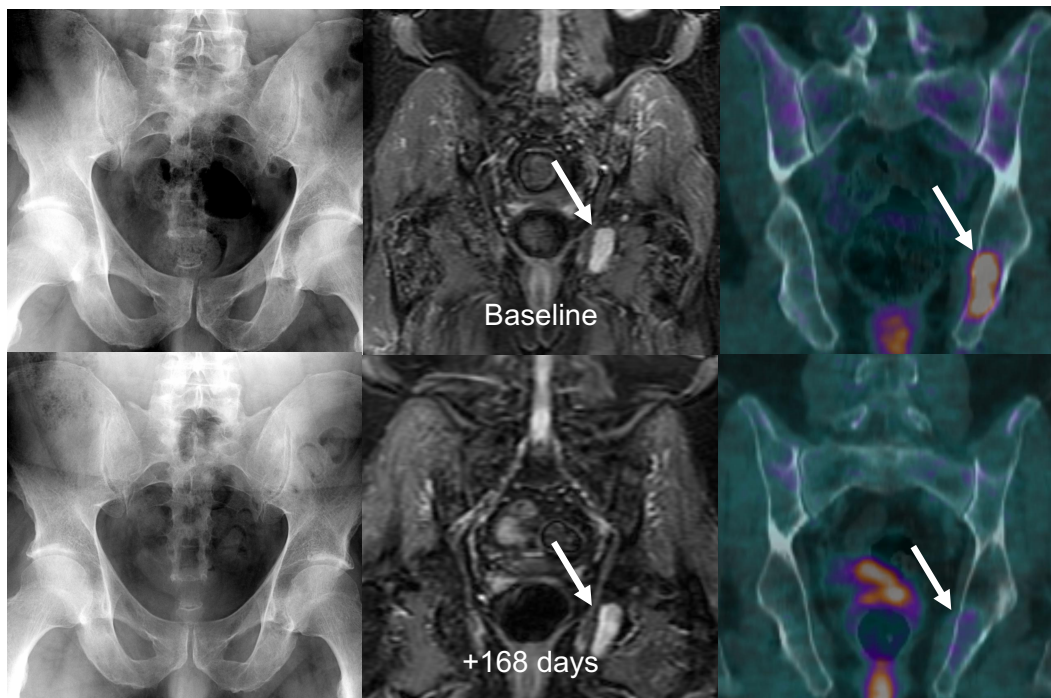


Figure 3. Untreated myeloma patient with time-concordant MBS, MRI, and FDG-PET/CT studies. Baseline imaging studies (top row) showed no osteolysis on MBS (top left), several foci on STIR-weighted MRI images with the largest in the left ischium (top middle), and 2 foci on FDG-PET/CT imaging (top right) with the largest again in the left ischium with a maximum SUV of 4.1. The patient was in near-complete remission 168 days later, with a significant decrease in focal activity in the left ischial lesion on PET (bottom right).

respectively (Figure 1H). The cumulative proportion of patients qualifying for MRI-defined CR (resolution of FL) was 29% at 18 months and reached 59% at 48 months. Among those without FL, MRI-defined CR (hypointensity on STIR images) was reached in 62% at 18 months, similar to the 56% attaining clinical CR status.

Figure 3 shows imaging sequences of a patient with stage IIIA IgA κ myeloma who in May 2005 was untreated when referred to our institution and enrolled in Total Therapy 3. Baseline MRI and FDG-PET/CT imaging studies showed active focal intramedullary disease. Approximately 6 months later, in October 2005, the patient had achieved n-CR status by laboratory criteria with near-complete resolution of abnormal FDG uptake on PET. The representative left ischial lesion's maximum SUV decreased from a baseline value of 4.1 to 1.2 and was considered resolved as the uptake was similar to background marrow activity, with resolution of PET-FL and suppression of FDG uptake (SUV-FL). Nearly 3 years later, the patient has retained n-CR status.

Posttreatment changes

Whereas early day 10 PET-CT changes did not affect outcome, complete FDG suppression in PET-FL and EMD before transplantation (but not clinical CR, not shown) conferred superior overall and event-free survival (Figure 1F). Thus, at 30 months from first autotransplantation, 92% and 89%, respectively, were alive and event-free compared with 71% and 63% among those with less than 100% suppression of FDG uptake in FL and EMD. When examined in the context of gene array-defined risk, complete FDG suppression before first transplantation conferred superior outcomes in both low-risk and high-risk groups, reaching statistical significance for overall survival in low-risk and for event-free survival in high-risk myeloma (Figure 1G). On multivariate analysis, normalization of PET findings before transplantation was associated with improved outcomes, whereas gene array-defined high-risk designation imparted poor overall and event-free

survival (Table 3). In the absence of molecular genetic data, the favorable implications of pretransplantation FDG suppression were opposed by elevated serum levels of LDH and B2M. Clinical CR or n-CR status before transplantation did not impact posttransplantation survival outcomes (Table 3).

Discussion

Herein, we demonstrate that several imaging parameters related to tumor burden, such as FL number assessed by MRI and PET, intensity of tumor metabolism (SUV-FL), and metastatic spread (EMD), all affect survival outcomes. Among 7 variables derived from 3 imaging methods, PET-FL was the one most highly correlated with 6 prognostic variables, all of which were individually linked to some of the other imaging parameters. Standard variables included B2M, LDH, and CRP. GEP-derived features included high-risk proliferation parameters and LB disease. According to logistic regression analysis, PET-FL was independently positively linked to 2 other imaging variables, MRI-FL and MBS-OL. Among the nonimaging parameters, PET-FL correlated positively with CRP and negatively with gene array-defined LB. Despite strong association with a series of established prognostic factors, PET-FL retained independent adverse prognostic implications along with the presence of CA and elevated LDH levels. PET-FL identified 30% of patients in whom, despite having low-risk disease as defined by GEP analysis, prognosis was inferior.

FDG suppression (SUV-FL) before transplantation was identified as an independent favorable prognostic variable, similar to published findings in well-studied malignancies such as malignant lymphoma, reflecting the importance of complete suppression of tumor metabolism in myeloma, regardless of gene array-defined risk, for durable disease control and survival. Absence of pretransplantation clinical CR as a favorable variable in the current survival model, previously linked to

Table 3. Multivariate Cox regression analyses of baseline laboratory and imaging parameters and FDG suppression prior to first transplantation associated with overall and event-free survival without and with gene array–derived parameters

Model	n/N (%)	Overall survival from first transplantation			Event-free survival from first transplantation		
		HR (95% CI)	P*	Cumulative R ² , percentage†	HR (95% CI)	P*	Cumulative R ² , percentage†
Multivariate without gene array data							
100% PET-FL reduction	140/196 (71)	0.33 (0.17-0.64)	.001	37.1	0.47 (0.26-0.85)	.013	48.1
PET-FL > 3	69/196 (35)	NS	NS	NS	2.01 (1.08-3.76)	.028	36.9
LDH ≥ 190 U/L	46/196 (23)	2.27 (1.11-4.65)	.024	43.0	2.61 (1.42-4.81)	.002	24.8
B2M > 5.5 mg/L	37/196 (19)	2.45 (1.19-5.02)	.015	48.6	2.00 (1.06-3.79)	.033	43.3
Multivariate with gene array data							
100% PET-FL reduction	126/175 (72)	0.41 (0.20-0.86)	.017	37.1	0.51 (0.27-0.96)	.038	56.2
GEP high-risk	28/175 (16)	2.64 (1.21-5.80)	.015	51.8	2.12 (1.07-4.23)	.032	48.1
Cytogenetic abnormalities	62/175 (35)	2.59 (1.18-5.72)	.018	58.5	NS	NS	NS
CRP ≥ 8 mg/L	57/175 (33)	2.43 (1.17-5.05)	.018	57.0	NS	NS	NS

HR indicates hazard ratio; CI, confidence interval; and NS, not statistically significant at the .05 level.

*P value from Wald χ^2 test in Cox regression. Multivariate model uses stepwise selection with entry level .1 and variable remains if it meets the .05 level. Variables considered for stepwise selection include albumin, beta-2-microglobulin (B2M), hemoglobin (Hb), lactate dehydrogenase (LDH), C-reactive protein (CRP), cytogenetic abnormalities (CA), and gene expression profiling (GEP) high-risk; imaging parameters include MRI-FL, MBS-OL, PET-FL, SUV-FL, and EMD. Variables considered for stepwise selection overall survival include B2M, Hb, LDH, CRP, CA, MRI-FL, MBS-OL, PET-FL, SUV-FL, EMD, PET-FL reduction, CR by first transplantation, and nCR by first transplantation. Variables considered for stepwise selection event-free survival include B2M, creatinine, Hb, LDH, CRP, CA, MRI-FL, MBS-OL, PET-FL, SUV-FL, EMD, PET-FL reduction, CR by first transplantation, and n-CR by first transplantation.

†Variable with smallest R² is first to enter model; the next smallest is second to enter. The largest R² is last to enter.

superior outcomes in high-risk myeloma,³⁵ attests to the greater prognostic power of FDG suppression encompassing myeloma cells that may not secrete monoclonal protein. In comprehensive analyses of GEP in Total Therapy 2 and Total Therapy 3, we also observed that losing CR status (“los-CR”) was a more powerful predictor of survival than not achieving CR (“non-CR”).³⁶

The prognosis of the 85% of patients with low-risk myeloma has been advanced markedly with Total Therapy 3, resulting in 4-year estimates of overall survival and event-free survival of 85% and 78%, respectively, including 90% with continued CR. However, the remaining 15% of patients presenting with high-risk myeloma still fare poorly with corresponding 4-year survival estimates of 45% and 37%, respectively, and a CR rate of 53%. The prognosis of high-risk patients not achieving complete FDG suppression was especially poor. Thus, our data support the use of serial PET examinations to individualize patient therapy and prompt changes to alternative therapies in those with persistent PET abnormalities, especially in the high-risk myeloma setting.

We previously reported that the superior clinical outcomes with Total Therapy 3 versus Total Therapy 2 were the result of the addition of bortezomib rather than greater compliance with intended therapies.³⁷ In addition to its well-documented antimyeloma effects, bortezomib has also been shown to stimulate osteoblasts.³⁸⁻⁴⁴ In its current front-line

trial comparing lenalidomide-dexamethasone with lenalidomide-dexamethasone plus bortezomib, the Southwest Oncology Group evaluates, via serial MRI and PET-CT scanning, whether the anticipated clinical benefit of bortezomib can be linked to faster onset and higher frequency of imaging-defined CR.

Acknowledgment

This work was supported by the National Cancer Institute, Bethesda, MD (Program Project grant CA55819).

Authorship

Contribution: B.B., J.D.S., F.v.R., E. Anaissie, R.W., J.E., and J.C. conceptualized the project; T.B.B., T.L.Y.B., E. Angtuaco, and R.W. performed imaging studies; T.A. collected data; J.H. and J.C. analyzed data; and T.B.B., T.L.Y.B., and B.B. wrote the paper.

Conflict-of-interest disclosure: The authors declare no competing financial interests.

Correspondence: Bart Barlogie, Myeloma Institute for Research and Therapy, 4301 West Markham St, #816, Little Rock, AR 72205; e-mail: barlogiebart@uams.edu.

References

- Dimopoulos MA, Mouloupoulos LA, Datsis I, et al. Imaging of myeloma bone disease. *Acta Oncol*. 2000;39:823-827.
- Lecouvet FE, Van de Berg BC, Malghem J, et al. Magnetic resonance and computed tomography imaging in multiple myeloma. *Semin Musculoskelet Radiol*. 2001;5:43-55.
- Mouloupoulos LA, Varma DG, Dimopoulos MA. Multiple myeloma: spinal MR imaging in patients with untreated newly diagnosed disease. *Radiology*. 1992;185:833-840.
- Roodman G. Mechanisms of bone metastasis. *N Engl J Med*. 2004;350:1655-1664.
- Yaccoby S, Pearce RN, Johnson CL, et al. Myeloma interacts with the bone marrow microenvironment to induce osteoclastogenesis and is dependent on osteoclast activity. *Br J Haematol*. 2002;116:278-290.
- Tian E, Zhan F, Walker R, et al. The role of the Wnt-signaling antagonist DKK1 in the development of osteolytic lesions in multiple myeloma. *N Engl J Med*. 2003;349:2483-2494.
- Walker R, Barlogie B, Haessler J, et al. Magnetic resonance imaging in multiple myeloma: diagnostic and clinical implications. *J Clin Oncol*. 2007; 25:1121-1128.
- Juwaid M, Cheson B. Positron-emission tomography in assessment of cancer therapy. *N Engl J Med*. 2006;354:496-507.
- Mahfouz T, Miceli M, Saghafifar F, et al. ¹⁸F-Fluorodeoxyglucose positron emission tomography contributes to the diagnosis and management of infections in patients with multiple myeloma: a study of 165 infectious episodes. *J Clin Oncol*. 2005;23:7857-7863.
- Spaepen K, Stroobants S, Dupont P, et al. Prognostic value of positron emission tomography (PET) with fluorine-18 fluorodeoxyglucose ([¹⁸F]FDG) after first-line chemotherapy in non-Hodgkin's lymphoma: is [¹⁸F]FDG-PET a valid alternative to conventional diagnostic methods? *J Clin Oncol*. 2001;19:414-419.
- Allal AS, Dulguerov P, Allaoua M, et al. Standardized uptake value of 2-[¹⁸F] fluoro-2-deoxy-D-glucose in predicting outcome in head and neck

- carcinomas treated by radiotherapy with or without chemotherapy. *J Clin Oncol*. 2002;20:1398-1404.
12. Smith IC, Welch AE, Hutcheon AW, et al. Positron emission tomography using [¹⁸F]-fluorodeoxy-D-glucose to predict the pathologic response of breast cancer to primary chemotherapy. *J Clin Oncol*. 2000;18:1676-1688.
 13. Weber WA, Petersen V, Schmidt B, et al. Positron emission tomography in non-small-cell lung cancer: prediction of response to chemotherapy by quantitative assessment of glucose use. *J Clin Oncol*. 2003;21:2651-2657.
 14. Weber WA, Ott K, Becker K, et al. Prediction of response to preoperative chemotherapy in adenocarcinomas of the esophagogastric junction by metabolic imaging. *J Clin Oncol*. 2001;19:3058-3065.
 15. Brucher BL, Weber W, Bauer M, et al. Neoadjuvant therapy of esophageal squamous cell carcinoma: response evaluation by positron emission tomography. *Ann Surg*. 2001;233:300-309.
 16. Maisey NR, Webb A, Flux GD, et al. FDG-PET in the prediction of survival of patients with cancer of the pancreas: a pilot study. *Br J Cancer*. 2000;83:287-293.
 17. Torizuka T, Tamaki N, Inokuma T, et al. Value of fluorine-18-FDG-PET to monitor hepatocellular carcinoma after interventional therapy. *J Nucl Med*. 1994;35:1965-1969.
 18. Haberkorn U, Strauss LG, Dimitrakopoulou A, et al. PET studies of fluorodeoxyglucose metabolism in patients with recurrent colorectal tumors receiving radiotherapy. *J Nucl Med*. 1991;32:1485-1490.
 19. Findlay M, Young H, Cunningham D, et al. Noninvasive monitoring of tumor metabolism using fluorodeoxyglucose and positron emission tomography in colorectal cancer liver metastases: correlation with tumor response to fluorouracil. *J Clin Oncol*. 1996;14:700-708.
 20. Vitola JV, Delbeke D, Meranze SG, et al. Positron emission tomography with F-18-fluorodeoxyglucose to evaluate the results of hepatic chemoembolization. *Cancer*. 1996;78:2216-2222.
 21. Angtuaco EF, Fassas AB, Walker R, et al. Multiple myeloma: clinical review and diagnostic imaging. *Radiology*. 2004;231:11-23.
 22. Barlogie B, Anaissie E, van Rhee F, et al. Incorporating bortezomib into upfront treatment for multiple myeloma: early results of total therapy 3. *Br J Haematol*. 2007;138:176-185.
 23. Barlogie B, Alexanian R, Pershouse M, Smallwood L, Smith L. Cytoplasmic immunoglobulin content in multiple myeloma. *J Clin Invest*. 1985;76:765-769.
 24. Sawyer J, Waldron J, Jagannath S, Barlogie B. Cytogenetic findings in 200 patients with multiple myeloma. *Cancer Genet Cytogenet*. 1995;82:41-49.
 25. Zhan F, Hardin J, Kordsmeier B, et al. Global gene expression profiling of multiple myeloma, monoclonal gammopathy of undetermined significance and normal bone marrow plasma cells. *Blood*. 2002;99:1745-1757.
 26. Shaughnessy J, Fenghuang Z, Kordsmeier B, Tian E, Smith R, Barlogie B. Gene expression profiling of the bone marrow microenvironment in patients with multiple myeloma, monoclonal gammopathy of undetermined significance and normal healthy donors. *Blood*. 2002;100:382a.
 27. Shaughnessy JD, Zhan F, Burington B, et al. A validated gene expression model of high-risk multiple myeloma is defined by deregulated expression of genes mapping to chromosome 1. *Blood*. 2007;109:2276-2284.
 28. Zhan F, Huang Y, Colla S, et al. The molecular classification of multiple myeloma. *Blood*. 2006;108:2020-2028.
 29. Blade J, Samson D, Reece D, et al. Criteria for evaluating disease response and progression in patients with multiple myeloma treated by high-dose therapy and haemopoietic stem cell transplantation. *Br J Haematol*. 1998;102:1115-1123.
 30. Durie BDM, Harousseau J-L, Miguel JS, et al. International uniform response criteria for multiple myeloma. *Leukemia*. 2006;20:1467-1473.
 31. Kaplan EL, Meier P. Nonparametric estimation from incomplete observations. *J Am Stat Assoc*. 1958;53:457-481.
 32. Mantel N. Evaluation of survival data and two new rank order statistics arising in its consideration. *Cancer Chemother Rep*. 1966;50:163-170.
 33. Cox DR. Regression models and life-tables. *J R Stat Soc [B]*. 1972;34:187-202.
 34. Gooley TA, Leisenring W, Crowley J, Storer BE. Estimation of failure probabilities in the presence of competing risks: new representations of old estimators. *Stat Med*. 1999;18:695-706.
 35. Haessler J, Shaughnessy JD Jr, Zhan F, et al. Benefit of complete response in multiple myeloma limited to high-risk subgroup identified by gene expression profiling. *Clin Cancer Res*. 2007;13:7073-7079.
 36. Hoering A, Crowley J, Shaughnessy J, et al. Complete remission in multiple myeloma examined as time-dependent variable in terms of both onset and duration in total therapy protocols. *Blood*. 2009;114(7):1299-1305.
 37. Pineda-Roman M, Zangari M, Haessler J, et al. Sustained complete remissions in multiple myeloma linked to bortezomib in total therapy 3: comparison with total therapy 2. *Br J Haematol*. 2008;140:625-634.
 38. Zangari M, Esseltine D, Cavallo F, et al. Predictive value of alkaline phosphatase for response and time to progression in bortezomib-treated multiple myeloma patients. *Am J Hematol*. 2007;82:831-833.
 39. Garrett IR, Chen D, Gutierrez G, et al. Selective inhibitors of the osteoblast proteasome stimulate bone formation in vivo and in vitro. *J Clin Invest*. 2003;111:1771-1782.
 40. Oyajobi BO, Garrett IR, Gupta A, et al. Stimulation of new bone formation by the proteasome inhibitor, bortezomib: implications for myeloma bone disease. *Br J Haematol*. 2007;139:434-438.
 41. Terpos E, Sezer O, Croucher P, Dimopoulos MA. Myeloma bone disease and proteasome inhibition therapies. *Blood*. 2007;110:1098-1104.
 42. Giuliani N, Morandi F, Tagliaferri S, et al. The proteasome inhibitor bortezomib affects osteoblast differentiation in vitro and in vivo in multiple myeloma patients. *Blood*. 2007;110:334-338.
 43. Mukherjee S, Raju N, Schoonmaker JA, et al. Pharmacologic targeting of a stem/progenitor population in vivo is associated with enhanced bone regeneration in mice. *J Clin Invest*. 2008;118:491-504.
 44. Qiang YW, Hu B, Chen Y, et al. Bortezomib induces osteoblast differentiation via Wnt-independent activation of β -catenin/TCF signaling. *Blood*. 2009;113:4319-4330.